Available online at www.sciencedirect.com

SciVerse ScienceDirect

Ceramics International 39 (2013) 2639–2643

CERAMICS INTERNATIONAL

www.elsevier.com/locate/ceramint

Hydrothermal synthesis of vanadium pentoxide nanostructures and their morphology control

Weijie Yu, Jinxing Wang*, Zhongping Gou, Wen Zeng, Weiwei Guo, Liyang Lin

College of Materials Science and Engineering, Chongqing University, Chongqing 400044, China

Received 16 July 2012; received in revised form 8 September 2012; accepted 8 September 2012
Available online 15 September 2012

Abstract

Different morphologies of vanadium pentoxide (V_2O_5) from 1D to 3D, including nanospheres, nanowires, urchin-like and flower-like nanostructures, have been synthetized by a simple hydrothermal method. Some parameters, such as the reaction temperature, the volume of polyvinyl pyrrolidone (PVP) and possible formation mechanisms of different V_2O_5 nanostructures were discussed. The results demonstrate that PVP and the reaction temperature play a critical role on the morphology of vanadium pentoxide.

Keywords: Morphology-controlling; V_2O_5 nanostructures; Hydrothermal; Formation mechanism

1. Introduction

As a layered structure, vanadium pentoxide V_2O_5 with an energy gap of 2.3 eV [1] have attracted great attention due to its novel properties such as lithium batteries [2,3] and gas sensor [4]. Thereby, V_2O_5 has been selected as a model system for the description of nanostructured materials [5,6]. Recently, various different nanostructures were synthetized by adding different inorganic or organic agents including hexamethylenetetramine (HMT) [7], cetyltrimethyl ammonium bromide (CTAB) [8,9], polyvinyl pyrrolidone (PVP) [10], $Cu(acac)_2$ [11]. Vanadium compounds such as $K_2V_8O_{21}$ [12], $LiNiVO_4$ [13], V(C,N) [14] were successfully synthetized by adding different agents. All the results suggest that surfactants play an important role on the morphologies and properties of the products. Usually, PVP polymer is regarded as the simplest crystal growth modifier, because it can selectively anchor on certain surfaces and thus kinetically control the growth rates of various planes [15]. In addition, PVP can also serve as a new class of reductants to kinetic control over both nucleation and growth [16]. Therefore, PVP is used as capping reagent owing to a strong interaction between the surfaces of nanocrystals and PVP based on the strong coordination ability of the O and N atoms in the pyrrolidone ring. It is believed that the selective adsorption of PVP on various crystallographic planes can effectively control and change the morphologies of the nanocrystals [17].

However, the effects of the PVP on the vanadium oxides morphology are investigated rarely, especially the volume of the PVP to the formation of vanadium pentoxides morphology and the reaction temperature. In this work, we used the so-called control variable method to prepare various morphologies of V_2O_5 nanocrystals. The main purpose of current work is to understand the effect of PVP on the formation of V_2O_5 nanostructures.

2. Experimental

2.1. Synthesis

Vanadium pentoxide (V_2O_5) was synthetized by a simple hydrothermal method in a Teflon-lined autoclave. So-called control variable method was used to prepare various morphologies of V_2O_5 nanocrystals. Experiment condition of different volumes of PVP at the same temperature and that of the same volume of PVP at different temperatures were adopted. In this work,

---

*Corresponding author. Tel./fax: +86 23 6510 2466.
E-mail address: wjx@cqu.edu.cn (J. Wang).

0272-8842/$ - see front matter Crown Copyright © 2012 Published by Elsevier Ltd and Techna Group S.r.l. All rights reserved.
http://dx.doi.org/10.1016/j.ceramint.2012.09.029

Table 1
Materials and synthetic conditions of different experimental programs.

Number	NH_4VO_4 (mol)	pH value	PVP (g)	Temperature (°C)
S1	0.003	2	0.15	180
S2	0.003	2	0.05	180
S3	0.003	2	0.15	140
S4	0.003	2	0.05	140

we designed four experimental programs named as a, b, c and d, respectively. Their detailed experimental parameters are shown in Table 1 and their detailed processes are as follows.

0.003 mol of ammonium metavanadate ($NH_4 \cdot VO_3$) was dissolved in distilled water containing 2 ml of 30% H_2O_2. Nitric acid was added dropwise to adjust the pH value of the solution to 2. After that, 0.15 g of analytical grade polyvingl pyrrolidone (PVP, K30) was added to the solution under vigorous magnetic stirrer to form a clear pure orange solution. Then, about 20 ml of the mixture was transferred to a 25 ml autoclave with a Teflon liner and maintained at 180 °C and 140 °C for 24 h, respectively. Afterwards, the resulting dark blue precipitates were washed with deionized water and anhydrous ethanol for several times and then dried at 60 °C in air for 10 h. The precipitate maintained at 180 °C was labeled as S1 and the other one maintained at 140 °C was labeled as S2.

For comparison, in other two experimental programs, the volume of polyvingl pyrrolidone (PVP, K30) was changed from 0.15 g to 0.05 g while other parameters were kept invariant. The resulting dark blue precipitate maintained at 180 °C was labeled as S3 and the other one maintained at 140 °C was labeled as S4. Finally, the precipitates in all reactions were calcined under 500 °C for 1 h.

2.2. Measurements

The structure and morphology of the precipitates were characterized by X-ray diffractometry (XRD) and field emission scanning electron microscopy (FE-SEM). A Rigaku D/Max-1200X diffractometry with the Cu Kα radiation operated at 30 KV and 100 mA was employed for the structure analysis. A Hitachi S-4300 SEM was employed for the surface morphologies observation.

3. Structural characterization and morphologies analysis

3.1. XRD analysis

Fig. 1 shows the XRD results of the calcined precipitates. The main diffraction peaks of 15.32°, 20.26°, 21.71°, 26.12°, 31.01°, respectively correspond to the characteristic diffraction of the (200), (001), (101), (110) and (301) planes of the vanadium pentoxide. The diffraction peaks match well with those of the standard V_2O_5 pattern (PDF no. 65-0131). This demonstrates that the precipitates of four experimental programs were pure V_2O_5 powder.

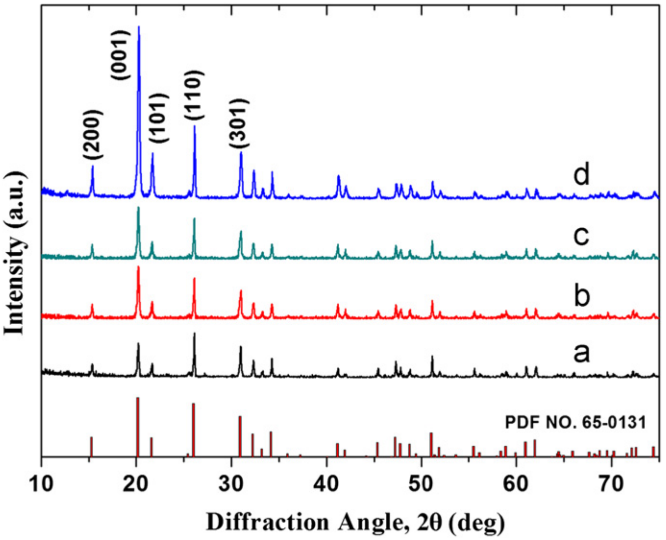

Fig. 1. XRD results of the four precipitates after calcined under 500 °C for 1 h at four programs: (a) S1 program (containing 0.15 g PVP at 180 °C), (b) S2 program (containing 0.15 g PVP at 140 °C), (c) S3 program (containing 0.05 g PVP at 180 °C), (d) S4 program (containing 0.05 g PVP at 140 °C).

3.2. SEM analysis

The morphologies of the samples of different programs were further investigated by FE-SEM. Four different morphologies of V_2O_5 nanostructures, including nanospheres, urchin-like, nanowires and nanoflowers, were obtained and showed in Fig. 2. One can see in Fig. 2(a) a large quantity of nanospheres were assembled of nanosheets. High resolution SEM observations reveal that these straight nanospheres are of width of ~2 μm and some of the nanosheets stick together (the inset image in Fig. 2(a)). Fig. 2(b) shows an urchin-like nanostructure of V_2O_5, which are composed of radially aligned nanorods. In a higher-magnification SEM image (the inset of Fig. 2(b)), it is clearly seen that the geometrical shapes of cross section of V_2O_5 are rectangular. The thickness and width of V_2O_5 nanorods are estimated to be 60~100 nm and 40~60 nm, respectively. The ends of the nanorods are regular. One can see in Fig. 2(c) a large quantity of nanowires. Their length and width are about several micrometers and ~100 nm, respectively. Along the nanowires, many particles adhere to the nanowires and some nanowires are broken. We suppose that the nanowires are broken by reason of heat treating at a high temperature. Fig. 2(d) shows flower-like V_2O_5 nanostructures which are assembled of petals. The diameter and thickness of the petals are about 1 μm and 60 nm, respectively.

4. Mechanism

In allusion to the four different morphologies of V_2O_5, including nanospheres, urchin-like, nanowires and nanoflowers, their formation mechanisms are discussed and the schematic representations are shown in Fig. 3.

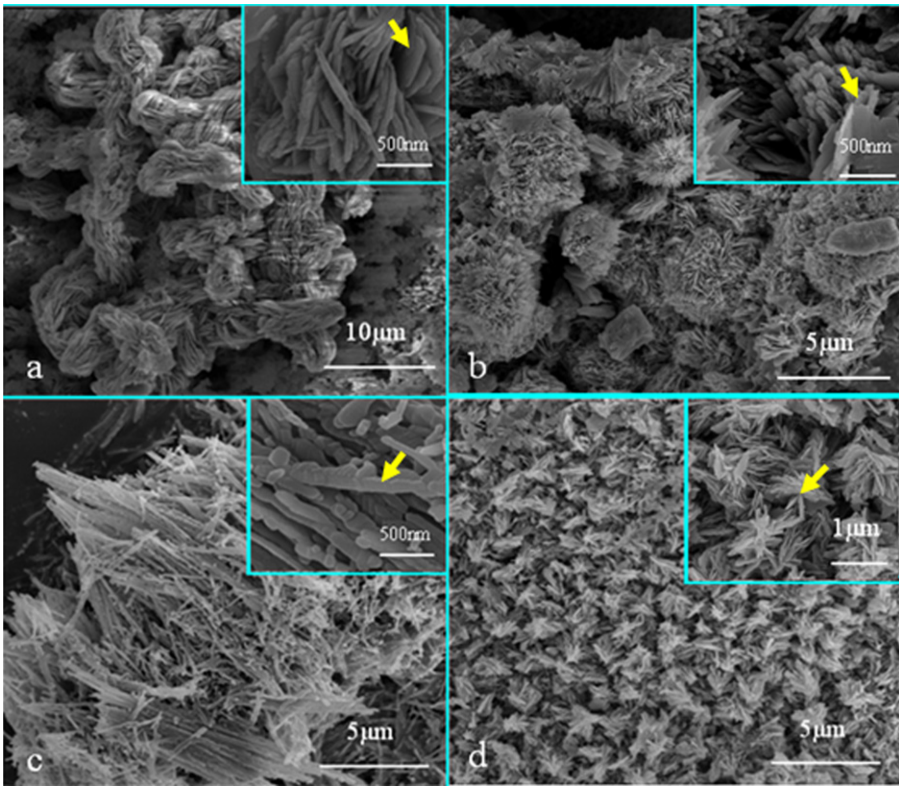

Fig. 2. Four different morphologies of V_2O_5 nanostructures obtained at: (a) S1 program (containing 0.15 g PVP at 180 °C), (b) S2 program (containing 0.15 g PVP at 140 °C), (c) S3 program (containing 0.05 g PVP at 180 °C), (d) S4 program (containing 0.05 g PVP at 140 °C).

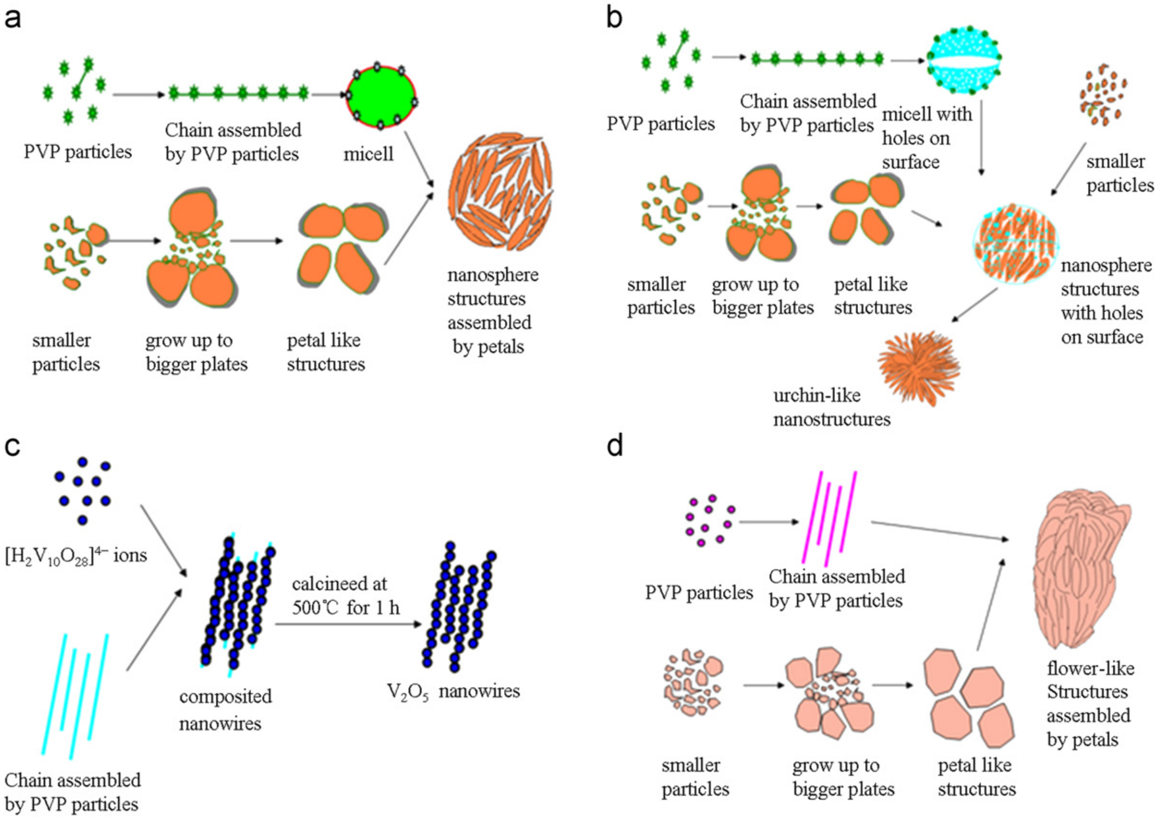

Fig. 3. Schematic representations of formation mechanisms of four different morphologies of V_2O_5 nanostructures: (a) nanospheres, (b) urchin-like, (c) nanowires and (d) nanoflowers.

Among these nanostructures, the formation mechanism of nanowires was discussed relatively more than those of the other nanostructures in previous works. In our work, V_2O_5 nanowires were also synthesized. As shown in Fig. 2(c), one can clearly see that a large number of V_2O_5 nanowires assemble into bundle-like nanostructures. Previously, V. Petkov and his co-workers [6] presented a new mechanism to explain the processes of $V_2O_5 \cdot nH_2O$ nanofibers. They also supposed that this mechanism was suitable for V_2O_5 nanowires. This new mechanism for V_2O_5 nanowires formation can be described as follows based on V. Petkov's interpretation [6]. If the coordination environment of V atoms in each bilayered slab is taken as octahedral (local distortion notwithstanding), the $[VO_6]$ octahedral shares edges to form double chains. These double chains then arrange in parallel and side by side via interchain V–O bonds (by sharing corners of octahedral) to form the slab. In this connectivity motif, intrachain V–O bonding is more extensive than interchain bonding. At the early stage of hydrothermal treatment of the aqueous solution of $H_2V_{10}O_{28}^{4-}$ ions [18,19], vanadium oxide fibers with large diameters can be formed along the interchain V–O bonds via a homogeneous nucleation. The basic reactions can be expressed as follows [20]:

$$NH_4 \cdot VO_3 + 4H_2O_2 \rightarrow NH_4[VO(O_2)_2] + 4H_2O + O_2 \quad (1)$$

$$NH_4[VO(O_2)_2] + H^+ \rightarrow H[VO(O_2)_2] + NH_4^+ \quad (2)$$

$$10H[VO(O_2)_2] \rightarrow [H_2V_{10}O_{28}]^{4-} + 4H_2O + 9O_2 \quad (3)$$

$$[H_2V_{10}O_{28}]^{4-} + 4NH_4^+ \xrightarrow{500^{\circ}C\ 1\ h} 5V_2O_5 + 3H_2O + 4NH_3 \quad (4)$$

During the reaction, the $[H_2V_{10}O_{28}]^{4-}$ ions gather along the chains which are assembled of the particles of PVP in the solution. In the course of the reaction, the PVP acts as a template as shown in Fig. 3(c).

As we know, PVP is a kind of template in which vinyl groups are hydrophobic while carbonyl groups are hydrophilic, which leads to the formation of chains and then leads to the formation of micells. Meanwhile, based on the agglomeration of the ions of $[H_2V_{10}O_{28}]^{4-}$ in the solution, the petal-like nanostructures nucleates. Finally, when these petal-like nanostructures gather in the micells, the nanospheres form as showed in Fig. 3(a). The formation for the space between sheets might result from the cleavage of vanadium oxide layers during the reaction process.

With the decrease of the volume of PVP from 0.15 g to 0.05 g, the morphology of nanospheres transform to the urchin-like nanostructures as shown in Fig. 2(b). The possible reason of the morphology transformation is believed to be related to the volume of PVP which can influence the formation of the petal-like structure of vanadium oxide. On one hand, when the volume of PVP is high, there are enough PVP particles to form micells in the solution to supply the positions in which the petal-like nanostructures can gather to form the nanospheres. On the other hand, when the volume of PVP is low, no enough PVP particles in the solution is available to form the micells. This leads to the formation of many holes on the surface of the formed micells. After that, the petal-like nanostructures gather in the micells with many holes on surfaces to form nanosphere nanostructures until the micells are filled full with the petal-like nanostructures. Finally, the $[H_2V_{10}O_{28}]^{4-}$ ions in the solution keep moving to the petal-like structures in the micells through the holes and the urchin-like nanostructures form as shown in Fig. 3(b).

When the volume of PVP is adjusted to 0.05 g and the hydrothermal treatment is carried out under 140 °C, the urchin-like nanostructures transform to flower-like nanostructures as shown in Fig. 2(d). The formation of the flower-like morphology is supposed to result from the intercalation, exfoliation and cleavage of the bulk vanadium oxides under hydrothermal treatment [5]. At the early stage of hydrothermal treatment in the aqueous H_2O_2 solution, the chains of PVP form as mentioned above in Fig. 2(c). We suppose that, due to the low reaction temperature, the PVP particles in solution can only used for chains assembling. Along these chains, the petal-like structures which are composed of the $[H_2V_{10}O_{28}]^{4-}$ ions start to grow and the novel three-dimensional flower-like nanostructures form as shown in Fig. 3(d).

5. Conclusions

In summary, V_2O_5 nanostructures of nanospheres, urchin-like, nannowires and flower-like morphologies have been successfully synthesized via polyvinyl pyrrolidone-assisted hydrothermal process. Herein, we found that the volume of PVP and the reaction temperature play important role in synthesizing a regular morphology of V_2O_5 nanostructures. Changing the volume of PVP or the reaction temperature will result in a tremendous change of the morphology of V_2O_5.

Acknowledgments

This work was supported by the China Fundamental Research Funds for the Central Universities (CDJZR10130011).

References

[1] M.N. Colpaert, Exploratory study of catalytic oxidation reactions on vanadium pentoxide single crystals, Zeitschrift für Physikalische Chemi 84 (1973) 1–4.

[2] C.K. Chan, H.L. Peng, R.D. Twesten, K. Jarausch, X.F. Zhang, Y. Cui, Fast, completely reversible Li insertion in vanadium pentoxide nanoribbons, Nano Letters 2 (2007) 490–495.

[3] M.R.J. Scherer, L. Li, P.M.S. Cunha, O.A. Scherman, U. Steiner, Enhanced electrochromism in gyroid-structured vanadium pentoxide, Advanced Materials 24 (2012) 1217–1221.

[4] J. Liu, X. Wang, Q. Peng, Y. Li, Vanadium pentoxide nanobelts: highly selective and stable ethanol sensor materials, Advanced Materials (Weinheim, Germany) 17 (2005) 764–767.

[5] G.C. Li, S.P. Pang, L. Jiang, Z.Y. Guo, Z.K. Zhang, Environmentally friendly chemical route to vanadium oxide single-crystalline

nanobelts as a cathode material for lithium-ion batteries, Journal of Physical Chemistry B 110 (2006) 9383–9386.

[6] V. Petkov, P.N. Trikalitis, E.S. Bozin, S.J.L. Billinge, T. Vogt, M.G. Kanatzidis, Structure of $V_2O_5 \cdot nH_2O$ xerogel solved by the atomic pair distribution function technique, Journal of the American Chemical Society 124 (2002) 10157–10162.

[7] W.W. Guo, T.M. Liu, L. Huang, H.J. Zhang, Q. Zhou, W. Zeng, HMT assisted hydrothermal synthesis of various ZnO nanostructures: structure, growth and gas sensor properties, Physica E 44 (2011) 680–685.

[8] C. Cao, Y. Gao, L. Kang, H. Luo, Self-assembly and synthesis mechanism of vanadium dioxide hollow microspheres, CrystEng-Comm. 12 (2010) 4048–4051.

[9] X.C. Jiang, Y.L. Wang, T. Herricks, Y.N. Xia, lf-assembly and synthesis mechanism of vanadium dioxide hollow microspheres, Journal of Materials Chemistry 14 (2004) 4048–4051.

[10] D. Zhu, H. Liu, L. Lv, Y.D. Yao, W.Z. Yang, Hollow microspheres of V_2O_5 and Cu-doped V_2O_5 as cathode materials for lithium-ion batteries, Scripta Materialia 9 (2008) 642–645.

[11] J.H. Huang, L.A. Gao, Anisotropic growth of $In(OH)_3$ nanotubes to nanorods and nanosheets via a solution-based seed method, Crystal Growth and Design 6 (2006) 1528–1532.

[12] J.N. An, C.Y. Xu, L. Zhen, Y.D. Huang, Surfactant-free hydrothermal synthesis and characterization of single-crystal $K_2V_8O_{21}$ nanobelts, Ceramics International 36 (2010) 1825–1829.

[13] C.H. Lu, S.J. Liou, Fabrication and microstructure of lithium nickel vanadium oxide prepared by solid-state reaction, Ceramics International 25 (1999) 431–436.

[14] C.L. Yeh, Y.D. Chen, Combustion synthesis of vanadium carbonitride from V-C powder compacts under nitrogen pressure, Ceramics International 33 (2007) 365–371.

[15] F. Bonet, K. Tekaia-Elhsissen, K.V. Sarathy, Study of interaction of ethylene glycol/PVP phase on noble metal powders prepared by polyol process, Bulletin of Materials Science 3 (2000) 165–168.

[16] Y. Sun, Y. Xia, Shape-controlled synthesis of gold and silver nanoparticles, Science 298 (2002) 2176–2179.

[17] C.V.S. Reddy, A.P. Jin, Preparation and characterization of $(PVP+V_2O_5)$ cathode for battery applications, Electrochemistry Communications 8 (2006) 279–283.

[18] B. Alonso, J. Livage, Synthesis of vanadium oxide gels from peroxovanadic acid solutions: A ^{51}V NMR study, Journal of Solid State Chemistry 148 (1999) 16.

[19] C.J. Fontenot, J.W. Wiench, M. Pruski, G.L. Schrader, Vanadia gel synthesis via peroxovanadate precursors. 1. in situ laser Raman and 51V NMR characterization of the gelation process, The Journal of Physical Chemistry B 104 (2000) 11622.

[20] T.C. Gujjarahalli, C. Pallellappa, A. Siddaramanan, L. Jacques, Morphological evolution of $(NH_4)_{0.5} \cdot V_2O_5 \cdot mH_2O$ fibers into belts, triangles, and rings, Inorganic Chemistry 50 (2011) 7421–7428.